

An Unusual (10,3)-a Racemic Twofold Interpenetrating Network Assembled from Isolable Tris(cyclopentadienyl)manganate and Cesocene Building Blocks

Sohrab Kheradmandan,^[a] Helmut W. Schmalle,^[a] Heiko Jacobsen,^[a] Olivier Blacque,^[a] Thomas Fox,^[a] Heinz Berke,^{*[a]} Mathias Gross,^[b] and Silvio Decurtins^[b]

Abstract: The syntheses and X-ray crystal structures of $[(18\text{-crown-6})_2\text{Cs}]^+[\text{Cp}_3\text{Mn}]^-$ (**1**), $[(18\text{-crown-6})_2\text{Cs}]^+[\text{Cp}'_3\text{Mn}]^-$ (**2**), $[\text{CsCp}']$ (**3**), $[(\text{CsCp}')_2(18\text{-crown-6})]$ (**4**), and $\text{Cs}[\text{MnCp}_3]$ (**5**), and the synthesis of $\text{Cs}[\text{MnCp}'_3]$ (**6**) are reported ($\text{Cp}' = \text{C}_5\text{H}_4\text{Me}$). The anions $[\text{Cp}_3\text{Mn}]^-$ (**1**⁻) and $[\text{Cp}'_3\text{Mn}]^-$ (**2**⁻) are characterized by η^2 coordination of all three Cp or Cp' rings. Measurements of the magnetic susceptibilities χ_M resulted

in values of $\mu_{\text{eff}} = 6.20\mu_B$ (300 K), $\mu_{\text{eff}} = 6.33\mu_B$ (301 K), and $\mu_{\text{eff}} = 5.83\mu_B$ (300 K) for **1**, **2**, and **5**, respectively, which are indicative of high-spin $d^5\text{-Mn}^{2+}$ centers. Density functional calculations illustrate that the coordination mode of **1**⁻ is

characteristic for its sextet electronic ground state. Compound **3** forms infinite chains of cesocene-type sandwiches in the solid state, which are broken up into small subunits by the addition of crown ether to form **4**. Compound **5** is a rare example of a (10,3)-a racemic interpenetrating network that crystallizes in the orthorhombic space group *Pbca*.

Keywords: coordination modes • density functional calculations • magnetic properties • metallocenes

Introduction

The first members of the manganocene family, bis(cyclopentadienyl)manganese, $[\text{MnCp}_2]$, and bis(methylcyclopentadienyl)manganese, $[\text{MnCp}'_2]$, have been known for more than 45 years.^[1] Their electronic properties, especially their high-spin/low-spin transition, have attracted a great deal of attention in the literature, and have been extensively studied by a wide variety of techniques, including photoelectron (PE),^[2] EPR,^[3, 4] and NMR spectroscopy,^[3, 5] magnetic measurements in solution,^[3] as well as X-ray structure analysis,^[6] and electron diffraction.^[7] Of all the metallocenes of the 3d elements, manganocenes possess the longest M–C distances. These complexes undergo facile ring-exchange reactions; a characteristic feature of ionic cyclopentadienyl complexes,^[8] which


allows a variety of substitutions of the Cp ligand by two-electron donors such as $\text{CO}^{[9]}$ or P(OR)_3 .^[10] Based on the easily performed Cp-substitution and adduct-formation reactions of manganocene derivatives, our synthetic efforts in the development of manganacumulenes with unusual magnetic and electronic properties^[11] utilize derivatives such as $[\text{Cp}'_2\text{Mn}(\text{dmpe})]$ ($\text{dmpe} = 1,2\text{-bis(dimethylphosphanyl)ethane}^{[12]}$ or $[\text{Cp}'(\text{dmpe})\text{Mn}]$ ($\text{Cp}' = \text{MeC}_5\text{H}_4$).^[13]

Recently, we have found that manganocene complexes are able to add another Cp ligand,^[14] which leads to the formation of the tris(cyclopentadienyl)manganate anion $[\text{Cp}_3\text{Mn}]^-$. The structural motif "MCp₃" is well established in main-group chemistry with a variety of different coordination geometries,^[15] but only a few examples exist in transition-metal chemistry.^[16] The tris(η^2 -cyclopentadienyl)manganate(II) anion $[\text{Cp}_3\text{Mn}]^-$ can thus be understood as the missing link in the series Cp_3Ti , Cp_3V , $[\text{Cp}_3\text{Mn}]^-$, which is characterized by a low electron count in conjunction with a low degree of hapticity.

We then set out to devise a rational synthesis for the previously unknown species tris(cyclopentadienyl)manganate. Since exploratory investigations showed that smaller cations such as Na^+ did not allow the formation of the $[\text{Cp}_3\text{Mn}]^-$ ion, it was assumed that for the stabilization of tris(cyclopentadienyl)manganate complexes, the presence of a large and presumably less coordinating cation is essential. The $[\text{Cp}_3\text{Mn}]^-$ and $[\text{Cp}'\text{Mn}]^-$ ions could, ultimately, be isolated and characterized as their cesium salts in the presence

[a] Prof. Dr. H. Berke, Dr. S. Kheradmandan, Dr. H. W. Schmalle, Dr. H. Jacobsen, Dr. O. Blacque, Dr. T. Fox
Anorganisch-Chemisches Institut der Universität Zürich
Winterthurerstrasse 190, 8057 Zürich (Switzerland)
Fax: (+41)1-635-6802

[b] Dr. M. Gross, Prof. Dr. S. Decurtins
Departement für Chemie und Biochemie, Universität Bern
Freiestrasse 3, 3012 Bern (Switzerland)

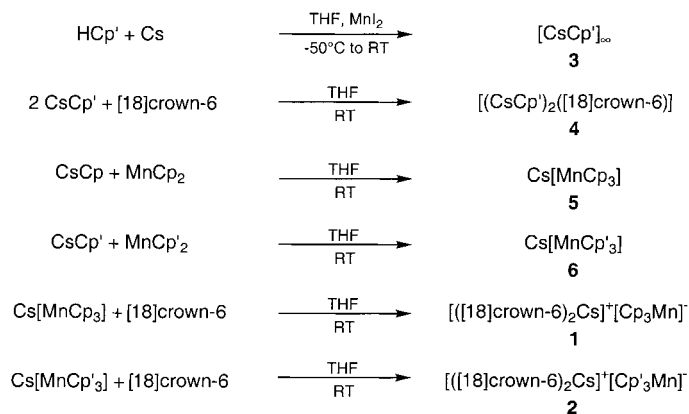
 Supporting information for this article is available on the WWW under <http://wiley-vch.de/home/chemistry/> or from the author. This includes optimized geometries, spin densities, and bonding energies, additional structural representations for the asymmetric units of **1** and **2**, a view along the independent chains and of their packing in **3**, and the herringbone packing motif in **4**.

of [18]crown-6: $[(\text{[18]crown-6})_2\text{Cs}]^+[\text{Cp}_3\text{Mn}]^-$ (**1**) and $[(\text{[18]crown-6})_2\text{Cs}]^+[\text{Cp}'\text{Mn}]^-$ (**2**). In this work, we report the syntheses and properties of the first paramagnetic high-spin complexes of the tris(cyclopentadienyl)manganate family. We describe the molecular geometry of the anions $[\text{Cp}_3\text{Mn}]^-$ (**1**[−]) and $[\text{Cp}'_3\text{Mn}]^-$ (**2**[−]), and present the results of density functional calculations on the anionic systems in various spin states.

During the course of our studies, we further isolated and characterized the compounds $[\text{CsCp}']$ (**3**) and $[(\text{CsCp}')_2(\text{[18]crown-6})]$ (**4**). Both represent examples of the most simple metallocene-sandwich complexes, a class of compounds for which structural properties,^[17] as well as chemical bonding,^[18] are still being investigated. Finally, we discuss the structure of $\text{Cs}[\text{MnCp}_3]$ (**5**), a compound that also contains triangular CpMn units, but forms a three-dimensional, racemic interpenetrating network.^[19, 20]

Results and Discussion

Syntheses: The first attempts to prepare the anion $[\text{Cp}'_3\text{Mn}]^-$ (**2**[−]; $\text{Cp}' = \text{MeC}_5\text{H}_4$) with Cs^+ as counterion in a stoichiometric one-pot reaction directly from Cs , MnI_2 , and Cp' proved to be unsuccessful. The reaction of three equivalents of methylcyclopentadienyl with four equivalents of cesium and one equivalent of manganese(II) iodide resulted in the polymeric compound $[\text{Cp}'\text{Cs}]_\infty$ (**3**), which is light pink in color and is comparable in many chemical respects to the related compound $[\text{CpCs}]_\infty$ (Scheme 1).^[21a] Here, excess cesium reduces



Scheme 1.

MnI_2 to give elemental manganese. The polymeric structure of **3** can be broken up upon addition of [18]crown-6 in THF; this leads to the formation of $[(\text{CsCp}')_2(\text{[18]crown-6})]$ (**4**; Scheme 1). Such motifs can indeed be entirely broken up, as demonstrated for $[\text{CsCp}(\text{[18]crown-6})]$.^[21b]

$[\text{Cp}'\text{Cs}]_\infty$ or $[\text{Cp}'\text{Cs}]$, prepared in situ, react with one equivalent of $[\text{Cp}'_3\text{Mn}]$ in THF to form the light pink, high-spin complex $\text{Cs}[\text{Cp}'_3\text{Mn}]$ (**6**; Scheme 1). In the same fashion, $\text{Cs}[\text{Cp}_3\text{Mn}]$ (**5**) is accessible from $[\text{CpCs}]$ and $[\text{Cp}_2\text{Mn}]$. It was not possible to specifically synthesize mixed-ligand complexes, such as $\text{Cs}[\text{Cp}_2\text{Cp}'\text{Mn}]$ or $\text{Cs}[\text{CpCp}'_2\text{Mn}]$, starting from

$[\text{CsCp}']$ and $[\text{MnCp}_2]$, or from $[\text{CsCp}]$ and $[\text{MnCp}'_2]$, respectively. In each case, we found complex product mixtures containing all possible combinations of $[\text{MnCp}_n\text{Cp}'_{3-n}]^-$ species ($n = 1, 2$), indicating the possibility of intermolecular exchanges of the Cp moieties. This may be due to the relatively small size of the 3d element manganese, since in the lanthanide series of larger elements the existence and isolation of mixed tricyclopentadienyl complexes is well established.^[22] Furthermore, the reaction between $[\text{MnCp}_3^*]$ ($\text{Cp}^* = \text{pentamethylcyclopentadienyl}$) and one equivalent of the $[\text{CsCp}]$, $[\text{CsCp}']$, or $[\text{CsCp}^*]$ compounds did not provide access to complexes of the kind $\text{Cs}[\text{Mn}(\text{Cp}_2^*)\text{L}]$, $\text{L} = \text{Cp}, \text{Cp}', \text{Cp}^*$. We believe that the steric requirements of the bulky Cp^* ligand are prohibitive to the formation of such compounds. Lastly, we should mention that the reactions between $[\text{CsCp}^*]$ and $[\text{MnCp}_2]$ or $[\text{MnCp}'_2]$ are not suitable for the synthesis of mixed-ligand complexes. In the latter case, a ring-exchange reaction was observed instead, resulting in $[\text{CsCp}']$ and $[\text{MnCp}_2^*]$, whereas in the former case, not only $[\text{MnCp}_2^*]$ was obtained, but also traces of **5**. The $[\text{MnCp}_2^*]$ was identified by ^1H NMR spectroscopy, showing a broad resonance at $\delta = 3.3$ in C_6D_6 at room temperature.^[23]

Since the light pink salts **5** and **6** show very low, or no solubility at all in THF or more polar solvents, we tried to exchange Cs^+ with other large cations, such as $[\text{NBu}_4]^+$ or $[\text{PPh}_4]^+$. The failure of such cation-exchange reactions led us to speculate that **5** and **6** form network structures in the solid state. An X-ray crystal structure analysis of **5** later confirmed our assumption, and, as we shall see later, it revealed unique structural properties. Only after the addition of the cyclic ether [18]crown-6 was it possible to obtain the compounds **1** and **2**, which were soluble in THF.

NMR properties: The complexes **1**, **2**, and **5** gave rise to ^1H -NMR spectra; however, owing to the paramagnetic nature of the compounds, the resonances for the protons of the Cp or Cp' units were broad and, as determined for **1** and **2**, temperature-dependent. The rather simple observed resonance patterns of the Cp and Cp' protons indicate dynamic behavior of the five-membered rings under the respective solvent and temperature conditions. For **6** it was impossible to obtain a ^1H NMR spectrum. The diamagnetic species **3** and **4** displayed distinct ^1H and ^{13}C NMR spectra at room temperature. Compound **4** showed signals for the Me groups and the two symmetry-distinguished types of protons or carbon atoms in the Cp' rings.

The ^{133}Cs NMR spectra of complexes **1**–**6** span a wide range of chemical shifts.^[24] The crown ether-embedded Cs^+ ions of **1** and **2** show the smallest difference in δ indicating their nearly-identical environment and their almost complete separation from the Mn centers. The observed Cs chemical shift difference of the diamagnetic Cp and Cp' derivatives **3** and **4** is greater than that of **1** versus **2**, but still in a range consistent with the same structural features being present in both compounds. In **5** and **6**, and **3** and **4** the Cs centers are assumed to have similar coordination spheres, therefore the chemical shifts of the earlier pair of complexes could in fact be related to paramagnetic influences.

Magnetic properties: The magnetic properties of the new complexes have been investigated by measurements of the susceptibility χ_M . From these results, an effective Bohr magneton of $\mu_{\text{eff}} = 6.20 \mu_B$ (300 K) and $\mu_{\text{eff}} = 6.33 \mu_B$ (301 K) could be deduced for compounds **1** and **2**, respectively. These values are a clear indication of the paramagnetic nature of these d⁵-Mn compounds, possessing a high-spin configuration with five unpaired electrons. Values greater than the spin-only value of d⁵ high-spin ($5.92 \mu_B$) may arise from an additional orbital angular moment based on the trigonal symmetry. For compound **5**, effective Bohr magnetons of $\mu_{\text{eff}} = 5.83 \mu_B$ (300 K), $5.85 \mu_B$ (200 K), $5.85 \mu_B$ (100 K), $5.53 \mu_B$ (10 K), $4.48 \mu_B$ (2 K) were established. These values once more indicate a d⁵ high-spin configuration. In contrast to compounds **1** and **2**, we additionally observe a decrease of the magnetic susceptibility at lower temperatures, as shown in Figure 1.

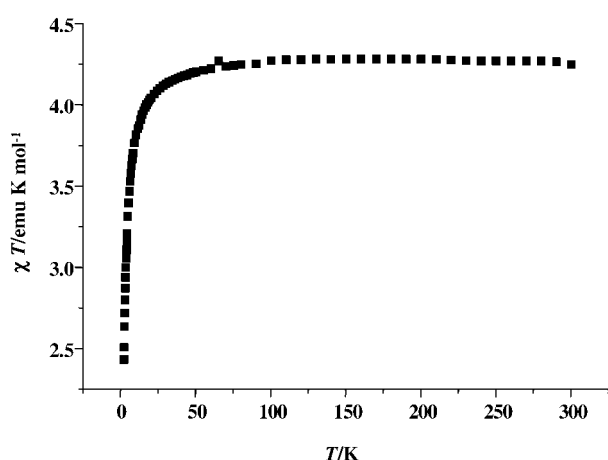


Figure 1. Magnetic susceptibility of **5**.

This behavior points to antiferromagnetic exchange between the manganese centers, occurring through the CpCs bridges. Since the solid-state structures of compounds **1**, **2**, and **5** could be determined by X-ray single-crystal analyses, we can relate the different magnetic behavior to structural properties. In the mononuclear complexes **1** and **2**, which possess isolated $[\text{Cp}_3\text{Mn}]^-$ and $[\text{Cp}'_3\text{Mn}]^-$ units, respectively, the Mn–Mn nonbonding distances amount to 13.3 and 14.2 Å. In contrast, for the network structure of **5**, a Mn–Mn bonding distance of only 10.7 Å has been established. Such close proximity of the manganese centers, together with the mediation of the CpCs bridges, cause the observed antiferromagnetic behavior. The unique solid-state structure of **5** will be discussed in detail later.

Molecular structures of the anions 1[−] and 2[−]: Single crystals of **1** and **2**, which were suitable for an X-ray structure analysis, were obtained from a THF/diethyl ether solution at -40°C . The corresponding anions **1[−]** and **2[−]** are displayed in Figure 2. In compounds **1** and **2**, the Cs⁺ counterion is sandwiched between two molecules of [18]crown-6. In the anion **1[−]**, the manganese center is coordinated to three cyclopentadienyl ligands in an η^2 fashion. The Mn1–C25, Mn1–C26, Mn1–C30,

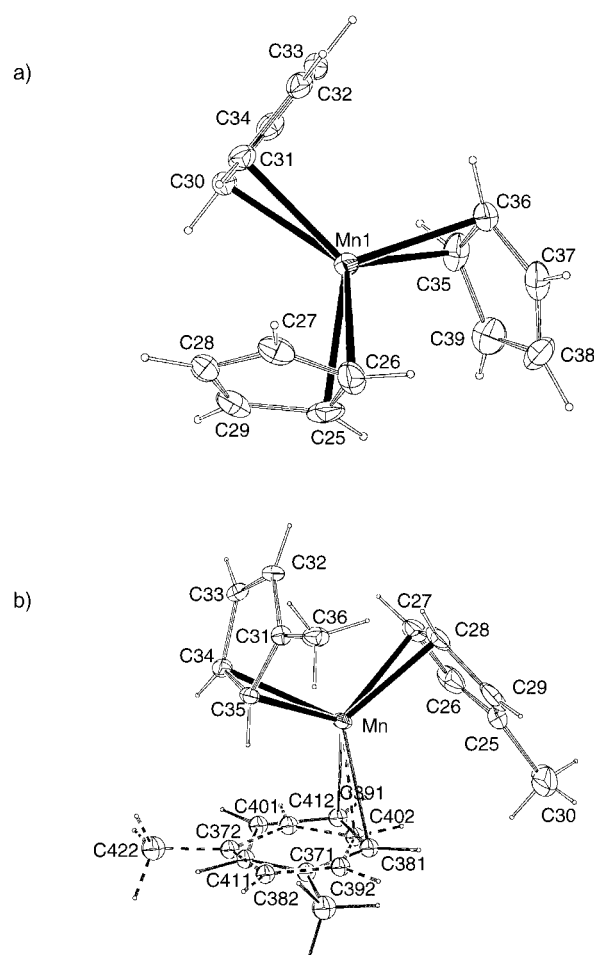


Figure 2. PLATON ellipsoid plot of a) **1[−]**, and b) **2[−]**. The probabilities are set to 30% (a), and 10% (b).

Mn1–C31, Mn1–C35, and Mn1–C36 separations (2.314(3), 2.406(3), 2.355(3), 2.359(3), 2.411(3), and 2.298(3) Å) span a rather large range of distances, which differ by up to 0.1 Å. These distances are comparable to those determined for the parent compound MnCp_2 ,^[6] a polymeric high-spin compound with bridging Cp units.

In the crystal, the anion **2[−]** shows one rotationally disordered Cp* ligand. This results in two independent molecular models for **2[−]**, which could be refined with fractional occupations of 0.56 and 0.44, respectively. In model **I**, the Mn–C27, Mn–C28, Mn–C34, Mn–C35, Mn–C381, and Mn–C391 distances are all in the same range (2.348(5), 2.331(5), 2.418(4), 2.356(3), 2.406(7), and 2.374(6) Å), comparable to that observed for **1[−]**. This leads to three pairs of C atoms, which coordinate each Cp' ring in an η^2 fashion to the metal center. For model **II**, we can deduce from the Mn–C separations that two η^2 -Cp' and one η^1 -Cp' ligands are present. The only possible carbon atom involved in η^1 coordination is C402, with a distance to the metal center of 2.283(9) Å. The rotation of the Cp' results in a Mn–C412 separation of 2.550(9) Å, and thus in the loss of one Mn–C bond. To address in more detail possible coordination modes of the anion $[\text{MnCp}_3]^-$, in connection with different spin states, we performed density functional (DFT) calculations that will be discussed in the next section.

DFT studies of $[\text{MnCp}_3]^-$: We carried out density functional calculations on various anionic d^5 complexes of the type $na-[\text{Mn}(\eta^x\text{-Cp})_3]^-$, with hapticities $x = 1, 2, 3, 5$, and total spin densities of na , $n = 1, 3, 5$. The relative energies of the calculated structures are summarized in Table 1.

We found the most stable molecule at 0 kJ mol^{-1} to be the sextet $5a-[\text{Mn}(\eta^2\text{-Cp})_3]^-$. The average Mn–C bonding distance of 2.37 \AA falls well within the range of the Mn–C separations observed in the crystal, and a spin density of $4.7a$ at the metal center indicates that the unpaired electrons are mainly localized in Mn d orbitals. The $\eta^2\text{-Cp}$ rings bind to the

Table 1. Relative energies [kJ mol^{-1}] of various anionic d^5 complexes of the type $na-[\text{Mn}(\eta^x\text{-Cp})(\eta^x\text{-Cp})(\eta^x\text{-Cp})]^-$.

	$3\eta^2$	$3\eta^1$	$2\eta^1\eta^5$	$2\eta^2\eta^1$	$\eta^1\eta^2\eta^5$	$2\eta^2\eta^5$
$n = 1$	215	223	—[c]	—[d]	113	119
$n = 3$	—[a]	—[b]	78	130	—[c]	92
$n = 5$	0	7	—[c]	2	—[c]	—[a]

[a] No local minimum could be optimized. [b] Converges to $2\eta^1\eta^5$ coordination. [c] No optimization attempted. [d] Converges to $\eta^1\eta^2\eta^5$ coordination.

metal center in a π -type interaction (Scheme 2a). A similar bonding mode with almost perpendicular M–C attachment is achieved by $\eta^1\text{-Cp}$ ligands (Scheme 2b), and the structural

alternatives $5a-[\text{Mn}(\eta^2\text{-Cp})_2(\eta^1\text{-Cp})]^-$ and $5a-[\text{Mn}(\eta^2\text{-Cp})(\eta^1\text{-Cp})_2]^-$ are calculated to be only 2 or 7 kJ mol^{-1} higher in energy, respectively.

This finding is in accord with the two independent molecular models found for 2^- in the X-ray structure analysis. The

next lowest energy structures at 78 and 92 kJ mol^{-1} are the intermediate spin cases $3a-[\text{Mn}(\eta^1\text{-Cp})_2(\eta^5\text{-Cp})]^-$ and $3a-[\text{Mn}(\eta^2\text{-Cp})_2(\eta^5\text{-Cp})]^-$, respectively. Here, one d orbital of Mn is doubly occupied, whereas another is empty. A typical π/π^* -bonding scheme becomes possible, thus inducing the ring of one Cp ligand slips into η^5 coordination. A similar coordination geometry is predicted for $1a-[\text{Mn}(\eta^2\text{-Cp})_2(\eta^5\text{-Cp})]^-$, a low-spin structure. Low-spin structures without one $\eta^5\text{-Cp}$ ligand are higher in energy by about 100 kJ mol^{-1} . Our calculations therefore suggest that the $3\eta^2$ coordination mode as observed in the crystal, is another manifestation of the electronic structure of complex 1^- , a $d^5\text{-Mn}$ complex possessing five singly occupied d orbitals.

Crystal structures of $[\text{CsCp}']$ (3**) and $[(\text{CsCp}')_2][18\text{crown-6}]$ (**4**):** The structure of $[\text{CsCp}']$ (**3**) consists of two distinct one-dimensional CsCp' chains, differing only in the position of the methyl groups, which are rotated relative to each other

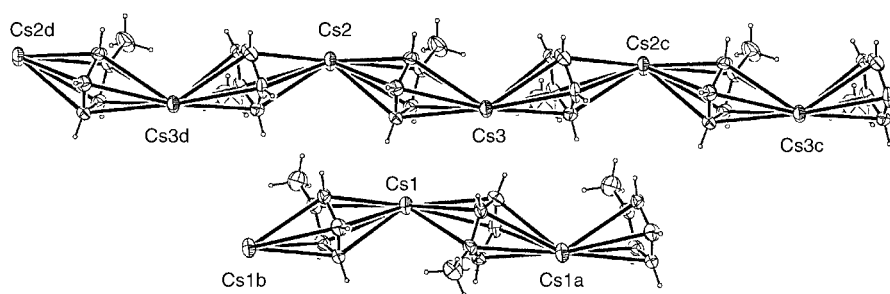


Figure 3. Structure of the two independent polymeric chains of **3** (50% probability PLATON ellipsoid plot).

(Figure 3). This one-dimensional polymeric chain, which consists of an infinite array of bent sandwiches, has already been found in the crystal structure of the similar $[\text{CsCp}]$ compound by high-resolution X-ray powder diffraction.^[21a] In one of the chains, Cs1 and Cp' alternate by means of the glide-plane symmetry along the a axis with methyl-carbon bonds in *anti* position along b or perpendicular to the glide plane a . This arrangement is illustrated in Scheme 3a.

The angle Cg–Cs1–Cg is 132.0° ; Cg is the center of gravity of the five C atoms of the Cp ring system. The other CsCp' chain also runs along the a direction of the unit cell in which two crystallographically independent Cs and Cp' groups [Cs2-Cp'2-Cs3-Cp'3] are arranged by a pseudo twofold axis. In this case, the dihedral angle between the methyl groups is about 45° and represents a *gauche* conformation (Scheme 3b). The two distinct Cg–Cs–Cg angles amount to 133.8° and 129.2° . The three different angles found in the crystal structure of **3** correspond well to those of $[\text{CsCp}]$ in which the chains are bent with a Cg–Cs–Cg angle of 129.7° .^[21a] On the other hand, the angle found in $[\text{PPh}_4][\text{Cp}_3\text{Cs}_2]$, for which the local environment of the Cs ions is similar, is somewhat smaller (115.6°).^[25] The η^5 -coordinated Cs atoms show Cs–C distances in the range $3.308(7)–3.355(6) \text{ \AA}$ for Cs1, $3.263(6)–3.423(7) \text{ \AA}$ for Cs2, and $3.275(7)–3.416(6) \text{ \AA}$ for Cs3. It is noteworthy that the two distinct polymeric chains are connected by weak interactions between each Cs atom and two carbon atoms of the closest Cp ring, resulting in a pseudo η^2 coordination. The closest intermolecular distance $\text{Cs} \cdots \text{C}$ of $3.742(7) \text{ \AA}$ found in **3** is somewhat longer than $3.699(5) \text{ \AA}$ as in $[\text{PPh}_4][\text{Cp}_3\text{Cs}_2]$ but smaller than the shortest distance of $3.765(6) \text{ \AA}$ in the crystal structure of $[\text{CpCs}]$.

The crystal structure of compound **4** (Figure 4) exhibits a complex metal-ligand connectivity of an infinite layer, in which the continuation of a $\text{Cp}'\text{-Cs-Cp}'$ two-dimensional network is terminated at both ends by $[18\text{crown-6}]$ molecules. There are, in addition, two noncoordinating THF molecules in the asymmetric unit of the cell. We also note that one of the methylcyclopentadienyl units displays positional disorder of the CH_3 group. The site occupation factors for the atoms of THF were set to $1/4$ due to the high displacement parameters found. The subunit of the network, which is about 23 \AA wide, consists of an open ellipse formed by the sequence of a $[(18\text{crown-6})\text{-Cs}(\text{Cp}'\text{-Cs})_5\text{-}(18\text{crown-6})]$ connectivity. One

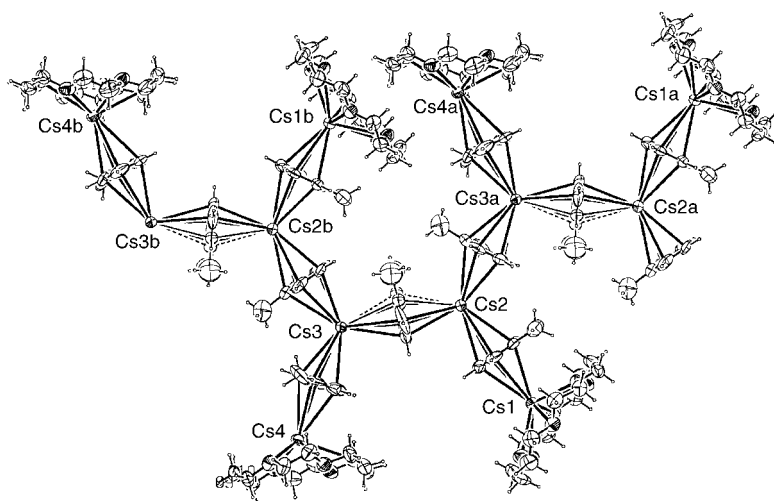


Figure 4. Structure of a representative section of the 2D network of **4** (50% probability PLATON ellipsoid plot; THF molecules are omitted for clarity).

ellipse shares two Cs–Cp'–Cs segments with two neighboring, intersecting ellipses that are rotated by 180° to form the opposite edge. This type of connectivity runs along the *b* direction of the cell. The central path of the separated networks can be interpreted as a sinusoidal connectivity of Cs–Cp'–Cs units. The network can also be described in a different way by considering an infinite number of chains of Cs1–Cp'–Cs2–Cp'–Cs3a–Cp'–Cs4, which are terminated at both ends by [18]crown-6 molecules. The approximately parallel-running chains are then connected by means of a ring, each non-terminal Cs atom having a $3\eta^5$ -Cp environment. Cs–Cp' distances vary between 3.291(11) and 3.396(11) Å. The mean Cs...Cs distances are 6.299(1) Å. The separated layers are packed in a herring-bone motif which can be seen in the *a,c* projection of the cell.

The interpenetrating network of Cs[MnCp₃] (5**):** Before we discuss the crystal structure of Cs[MnCp₃] (**5**) in more detail, we will begin with a few general remarks regarding (10,3) and (10,3)-a networks. The basic ideas and classification of multidimensional networks may be traced back to the classical work of Wells.^[19] In this series of papers, he describes the three-dimensional, three-connected decagonal net. He assigns the (10,3) net to the cubic space groups *I*₄/3 and *I*₄/amd, which are noncentrosymmetric and centrosymmetric, respectively. The nomenclature (10,3) is such that the first number describes the number of subunits forming one independent ring, whereas the second number stands for the degree of branching at every point of connectivity. The noncentrosymmetric situation most probably represents the symmetry for interpenetrating nets of the same chirality, whereas the centrosymmetric case allows for interpenetration of nets with opposite chiralities. Wells also postulates that (10,3)-a interpenetrating-network structures of identical nets may be observed with the same handedness, which would be the case for noncentrosymmetric space groups, such as *P*₂/3, *P*₄/32, or *P*₄/32.^[20] In centrosymmetric space groups, the interpenetrating nets may be considered as a three-dimensional racemate of opposite handedness. An even more

complex structure was presented by Abrahams and co-workers,^[26] in which four right- and four left-handed enantiomorphic interpenetrating (10,3)-a networks form a Wellsian three-dimensional racemate in the centrosymmetric space group *Fd* $\bar{3}$ *c*.

Keper and Rosseinsky^[27] found quadruple interpenetration of the (10,3)-a network in all four nets. In their structure, hydrogen bonding results in the separation of nets of the same handedness. An excellent review in the field of supramolecular chemistry, focussing on interpenetrating one-, two- and three-dimensional network

structures, was recently presented by Batten and Robson.^[28]

A twofold interpenetration of racemic three-dimensional nets is another rare example where noncovalent interactions build up a centrosymmetric, three-dimensional structure.^[29] Noninterpenetrating (10,3)-a chiral network structures were found to crystallize in the noncentrosymmetric cubic space groups, such as *P*₂/3, *P*₄/32, *P*₄/32. Finally, we note that, for a 1,2-dithiooxalate-bridged three-dimensional net, the orthorhombic space group *P*₂/2₁ is appropriate.^[30]

Compound **5** is another rare example of a (10,3)-a network, which crystallizes in the orthorhombic space group *Pbca*, of which *P*₂/2₁ is the noncentrosymmetric subgroup. The three-dimensional structure of **5** exhibits a network of metal decagons, and still contains triangular [MnCp₃] units. It is connected in an alternating fashion by cesium centers, possessing a local T-shaped coordination. These two structural motifs are displayed in Figure 5a and 5b, respectively.

Two neighboring manganese and cesium centers establish the connection to another fused decagon. This way, the indefinitely connected manganese and cesium units form helical strands propagating in all three dimensions. Within one framework, the helices possess the same helicity, and form a three-dimensional optical isomer according to the space group symmetry *P*₂/2₁ (Figure 6a). The superposition of this substructure and its optical counterpart results in the interpenetrating net shown in Figure 6b. Both enantiomers interpenetrate each other in the centers of the decagons.

To simplify this complex situation, a stereoview of the (10,3)-a nets, in which the Cp rings have been replaced by their centers of gravity, is presented in Figure 7.

We can see that the two networks are interconnected in a chain-link fashion, in which each decagon is penetrated by exactly one of its enantiomorphs.

Conclusion

In this work, we have introduced new representatives of main-group and transition-metal cyclopentadienyl complexes. The

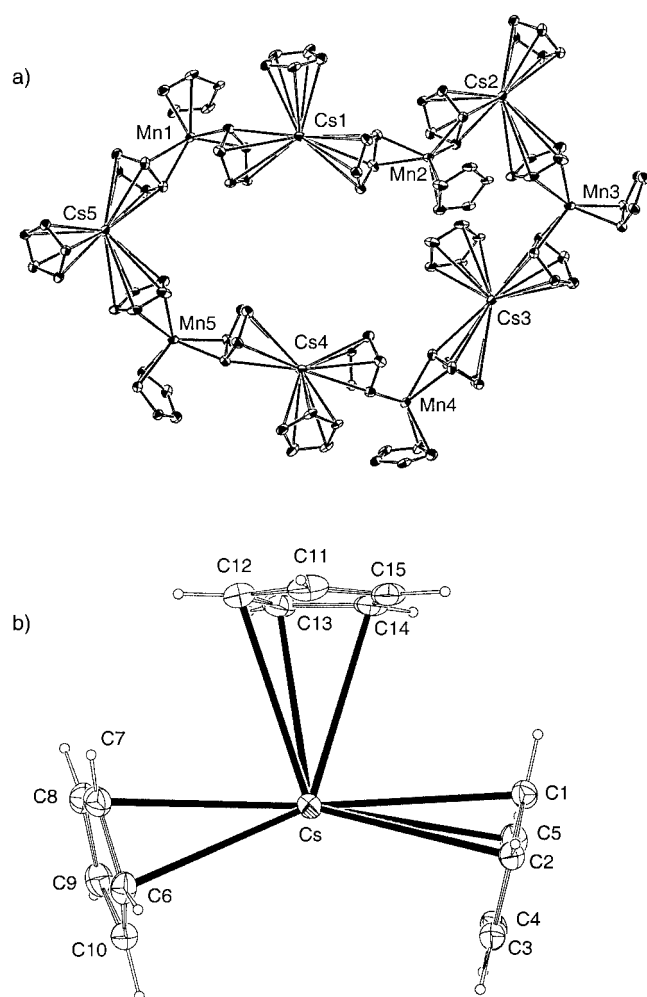


Figure 5. PLATON ellipsoid plots of the $[-\text{Mn}(\eta^2\text{-Cp})\text{-Cs}(\eta^2\text{-Cp})]_5$ decagon (a), and the T-shaped coordination of the Cs centers (b) in the network structure of **5**. The probabilities are set to 50% (a), and 30% (b).

anions $[\text{Cp}_3\text{Mn}]^-$ (**1**[−]) and $[\text{Cp}'_3\text{Mn}]^-$ (**2**[−]) are characterized by η^2 coordination of all three Cp and Cp' rings, and possess a high-spin electronic configuration. $[\text{Cp}'\text{Cs}]$ (**3**) forms infinite chains of cesocene-type sandwiches in the solid state, which are broken up into small subunits by the addition of crown

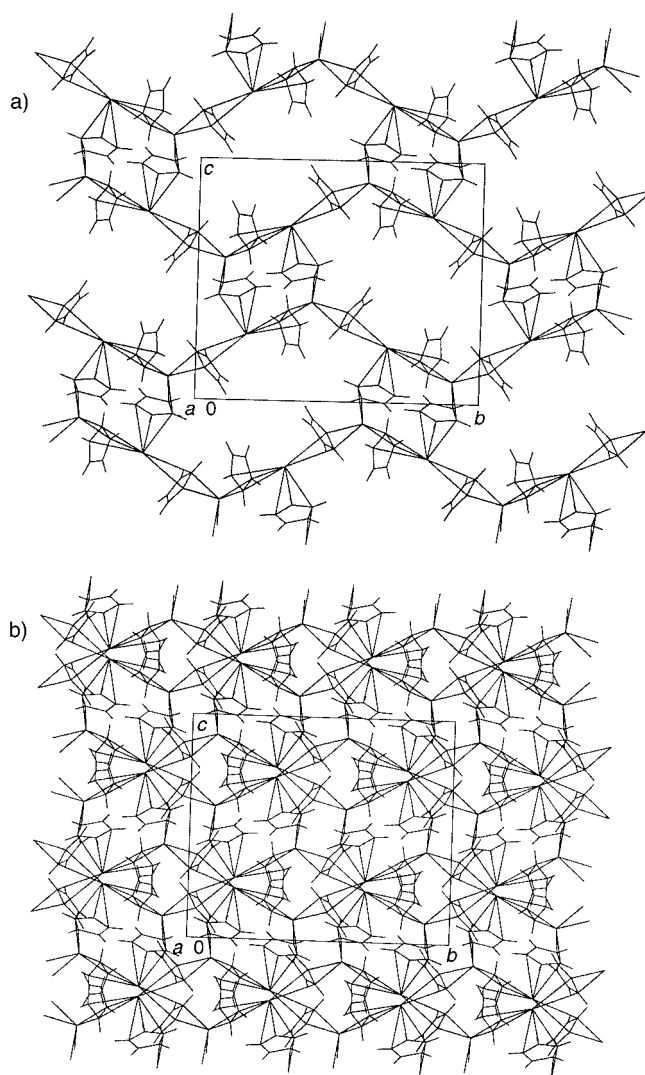


Figure 6. PLUTON wire model in b,c projection of the unit cell for the substructure of one network with space group symmetry $P2_12_1$ (a), and the full structure of **5** according to the space group Pbc_a (b).

ether. Combining the two units MnCp_3 and CsCp leads to the formation of an unusual, (10,3)-a racemic interpenetrating network.

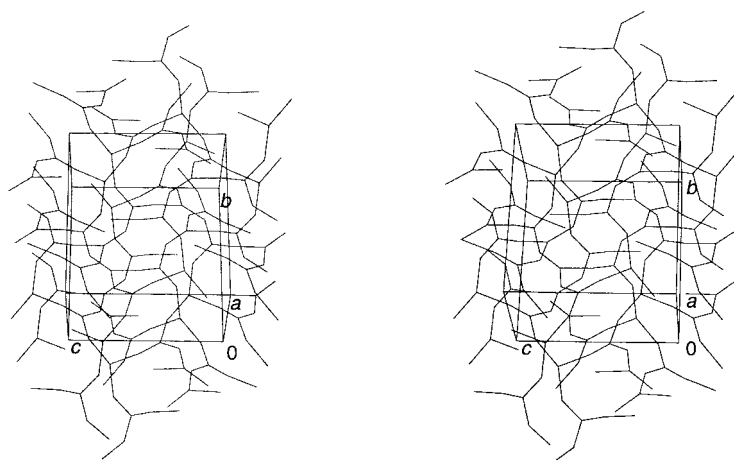


Figure 7. Structure of a section of the 3D network structure of **5** (PLUTON stereoplot; Cp rings are represented by their centers of gravity).

Experimental Section

Synthetic procedures: All operations were carried out under an atmosphere of N_2 , using standard Schlenk and glovebox techniques. $[\text{Cp}_2\text{Mn}]$ was prepared according to reference [1] and CpCs was obtained as described by Olbrich et al.^[21]

$[(18\text{-crown-6})_2\text{Cs}]^+[\text{Cp}_3\text{Mn}]^-$ (1**):** Compound **5** (0.1 mmol) was suspended in THF (10 mL) at room temperature, and treated with 18-crown-6 (0.2 mmol). After 20 min, the solvent was removed and the product washed with diethyl ether. Recrystallization from THF/diethyl ether at -30°C afforded colorless or light pink crystals

in quantitative yields. ^1H NMR (300 MHz, $[\text{D}_8]\text{THF}$, 30°C , TMS): $\delta = 3.5$ (s, 48H; $[\text{18}]\text{crown-6}$), 51.6 (br, 15H; C_5H_5) ppm; ^1H NMR (300 MHz, $[\text{D}_8]\text{THF}$, 40°C , TMS): $\delta = -3.4$ (s, 9H; CH_3), 3.6 (s, 48H; $[\text{18}]\text{crown-6}$), 25.6 (br, 12H; C_5H_4) ppm; (300 MHz, $[\text{D}_8]\text{THF}$, 50°C , TMS): $\delta = -3.0$ (s, 9H; CH_3), 3.6 (s, 48H; $[\text{18}]\text{crown-6}$), 24.8 (br, 12H; C_5H_4) ppm; ^{133}Cs NMR (65.615 MHz, $[\text{D}_8]\text{THF}$, 20°C , CsI in D_2O ext.): $\delta = 164.4$ (s); elemental analysis calcd (%) for $\text{C}_{39}\text{H}_{63}\text{CsMnO}_{12}$ (911.764): C 51.38, H 6.96; found: C 51.34, H 6.64; $\mu_{\text{eff}} = 6.20 \mu_{\text{B}}$ (300 K), $6.13 \mu_{\text{B}}$ (199 K), $6.02 \mu_{\text{B}}$ (99 K) $5.81 \mu_{\text{B}}$ (10 K).

$[(\text{18crown-6})_2\text{Cs}]^+[\text{Cp}^-\text{Mn}]^-$ (2): This compound was prepared from **6** and $[\text{18}]\text{crown-6}$ in an analogous procedure to that described for **1**. ^1H NMR (300 MHz, $[\text{D}_8]\text{THF}$, 30°C , TMS): $\delta = -4.12$ (br, 9H; $\text{CH}_3\text{C}_5\text{H}_4$), 3.60 (s, 48H; $[\text{18}]\text{crown-6}$), 26.0 (br, 12H; $\text{CH}_3\text{C}_5\text{H}_4$) ppm; (300 MHz, $[\text{D}_8]\text{THF}$, 45°C , TMS): $\delta = 3.5$ (s, 48H; $[\text{18}]\text{crown-6}$), 54.0 (br, 15H; C_5H_5) ppm; ^{133}Cs NMR (65.615 MHz, $[\text{D}_8]\text{THF}$, 20°C , CsI in D_2O ext.): $\delta = 156.0$ (s) ppm; elemental analysis calcd (%) for $\text{C}_{42}\text{H}_{69}\text{CsMnO}_{12}$ (953.845): C 52.89, H 7.29; found: C 52.81, H 7.05; $\mu_{\text{eff}} = 6.33 \mu_{\text{B}}$ (301 K), $6.22 \mu_{\text{B}}$ (199 K), $6.01 \mu_{\text{B}}$ (98 K) $5.78 \mu_{\text{B}}$ (10 K).

$[\text{Cp}^-\text{Cs}]$ (3): Metallic cesium (177.3 mg, 1.33 mmol) was covered with THF at -40°C , and Cp^-H (82 mg, 1.0 mmol) was added. The resulting suspension was warmed to room temperature, and then cooled down to -10°C , while MnI_2 (100 mg, 0.33 mmol) was added. The reaction mixture was warmed once again to room temperature, and heated under reflux for 15 h. The resulting violet solution was filtered, and the solvent removed under high vacuum. Recrystallization from THF/pentane at -30°C afforded **3** (170 mg) as light pink crystals (80% yield with respect to Cp^-H). ^1H NMR (500.23 MHz, $\text{C}_4\text{D}_8\text{O}$, 30°C): $\delta = 2.04$ (s, 3H; $\text{CH}_3\text{C}_5\text{H}_4$), 5.22 (t, $J_{\text{H,H}} = 2$ Hz, 2H; C_5H_4), 5.29 (t, $J_{\text{H,H}} = 2$ Hz, 2H; C_5H_4) ppm; $^{13}\text{C}\{^1\text{H}\}$ NMR (125.8 MHz, $\text{C}_4\text{D}_8\text{O}$, 40°C): $\delta = 15.5$ (s; CH_3), 106.5 (s; C_5H_4), 107.9 (s; C_5H_4), 116.3 (s; C_{ipso}) ppm; ^{133}Cs NMR (65.615 MHz, $\text{C}_4\text{D}_8\text{O}$, 22°C): $\delta = 312$ (s) ppm; elemental analysis calcd (%) for $\text{C}_6\text{H}_7\text{Cs}$ (212.03): C 33.99, H 3.33; found: 33.84, H 3.16.

$(\text{Cs})_2(\text{18crown-6})$ (4): Compound **3** (127.2 mg, 0.2 mmol) and $[\text{18}]\text{crown-6}$ (106.0 mg, 0.4 mmol) were mixed in THF (5 mL) at room temperature. After 20 min the solvent was decanted off. The raw product was washed with pentane. Recrystallization from THF/pentane at -30°C yielded light pink crystals of **4** (135 mg, 98%). ^1H NMR (500.23 MHz, $\text{C}_4\text{D}_8\text{O}$, 30°C):

$\delta = 2.1$ (s, 3H; C_5H_4), 3.5 (s, 48H; $[\text{18}]\text{crown-6}$), 5.27 (t, $J_{\text{H,H}} = 2$ Hz, 2H; C_5H_4), 5.34 (t, $J_{\text{H,H}} = 2$ Hz, 2H; C_5H_4); $^{13}\text{C}\{^1\text{H}\}$ NMR (125.8 MHz, $\text{C}_4\text{D}_8\text{O}$, 30°C): $\delta = 16.2$ (s; C_5H_4), 70.9 (s; $[\text{18}]\text{crown-6}$), 105.7 (s; C_5H_4), 107.1 (s; $\text{CH}_3\text{C}_5\text{H}_4$), 115.3 (C_{ipso}) ppm; ^{133}Cs NMR (65.615 MHz, $\text{C}_4\text{D}_8\text{O}$, 25°C): $\delta = -244.7$ (s) ppm; elemental analysis calcd (%) for $\text{C}_{24}\text{H}_{28}\text{O}_6\text{Cs}_2$ (688.38): C 41.88, H 5.56; found: C 42.08, H 5.18.

$[\text{CsMnCp}]$ (5): A solution of $[\text{MnCp}]$ (185.1 mg, 1.0 mmol) in THF (10 mL) was mixed with a solution of CsCp (1.0 mmol, 10 mL) in THF. Immediately, slightly pink microcrystals began to precipitate. After 15 min, the solvent was decanted off, and the solid washed two or three times with THF. After further washing with diethyl ether, the product **5** was dried in vacuo; yield 345 mg (90%). ^1H NMR (500.23 MHz, $\text{C}_4\text{D}_8\text{O}$, 30°C): $\delta = 51.6$ (br; C_5H_5) ppm; ^{133}Cs NMR (65.615 MHz, CD_3CN , 20°C): $\delta = -3.7$ (s) ppm; elemental analysis calcd (%) for $\text{C}_{15}\text{H}_{15}\text{CsMn}$ (383.13): C 47.02, H 3.95; found: C 46.97, H 3.72; $\mu_{\text{eff}} = 5.83 \mu_{\text{B}}$ (300 K), $5.85 \mu_{\text{B}}$ (200 K), $5.85 \mu_{\text{B}}$ (100 K), $5.53 \mu_{\text{B}}$ (10 K), $4.48 \mu_{\text{B}}$ (2 K).

$[\text{CsMn}]$ (6): A solution of Mn (213.2 mg, 1.0 mmol) in THF (10 mL) was treated with a solution of Cs (1.0 mmol, 10 mL) in THF. Work-up was carried out as described for **5**. Yield 364 mg (95%); ^{133}Cs NMR (65.615 MHz, CD_3CN , 20°C): $\delta = 55$ (s) ppm; elemental analysis calcd (%) for $\text{C}_{18}\text{H}_{21}\text{CsMn}$ (425.21): C 50.82, H 4.89; found: C 50.81, H 4.83.

X-ray crystal structure analyses: The X-ray diffraction data were collected at 183(1) K for compounds **1** to **4**, and at 123(1) K for **5**, using an imaging plate detector system (Stoe IPDS) with graphite-monochromated $\text{MoK}\alpha$ radiation. A total of 200, 167, 200, 251, and 167 images were exposed at constant times of 2.50, 2.50, 6.00, 4.00, and 2.00 min per image for the structures **1**–**5**, respectively. The crystal-to-image distances were set to 50 mm for all of the five compounds ($\theta\text{-max} = 30.31$ to 30.34°). ϕ -rotation for **1**, **2**, and **5**, and oscillation modes for **3** and **4** were used for the increments of 1.2, 1.2, 1.0, 0.8, and 1.2° per exposure in each case. Total exposure times were 22, 19, 34, 34, and 17 h. The intensities were integrated by using a dynamic peak profile analysis, and an estimated mosaic spread (EMS) check was performed to prevent overlapping intensities. A total of 8000 reflections for **3**, **4**, and **5**, and 7998 reflections for **1** and **2** were selected out of the whole limiting sphere with intensities $I > 6\sigma(I)$ for the cell-parameter refinement. A total of 30770, 54775, 23789, 79541, and 30617 reflections were collected, of which 11796, 13011, 5903, 20122, and

Table 2. Crystallographic data for **1**–**5**.

	1	2	3	4	5
formula	$\text{C}_{39}\text{H}_{63}\text{CsMnO}_{12}$	$\text{C}_{42}\text{H}_{69}\text{CsMnO}_{12}$	$\text{C}_{18}\text{H}_{21}\text{Cs}_3$	$\text{C}_{100}\text{H}_{160}\text{Cs}_8\text{O}_{25}$	$\text{C}_{15}\text{H}_{15}\text{MnCs}$
color	light pink	pink	light pink	pink	colorless
crystal dimensions [mm]	$0.32 \times 0.24 \times 0.11$	$0.32 \times 0.24 \times 0.11$	$0.21 \times 0.17 \times 0.05$	$0.78 \times 0.56 \times 0.53$	$0.51 \times 0.44 \times 0.32$
crystal system	triclinic	monoclinic	monoclinic	orthorhombic	orthorhombic
space group (no.)	$P\bar{1}$ (2)	$P2_1/n$ (14)	$P2_1/a$ (14)	$P2_12_12_1$ (19)	$Pbca$ (61)
a [Å]	11.8868(9)	16.6927(9)	11.3746(7)	13.9493(6)	10.7523(6)
b [Å]	13.6526(10)	16.5696(12)	19.7533(12)	18.9321(8)	17.2570(13)
c [Å]	15.6473(12)	17.0119(9)	9.0207(6)	25.5013(17)	14.9678(8)
α [°]	104.484(8)	90	90	90	90
β [°]	107.242(9)	96.351(6)	91.395(8)	90	90
γ [°]	106.417(9)	90	90	90	90
V [Å ³]	2166.3(3)	4676.5(5)	2026.2(2)	6734.6(6)	2777.3(3)
Z	2	4	4	2	8
F_w	911.74	953.82	636.08	1412.78	383.12
ρ_{calcd} [g cm ⁻³]	1.398	1.355	2.085	1.393	1.833
absorption coefficient [mm ⁻¹]	1.189	1.105	5.362	2.195	3.509
$F(000)$	946	1988	1176	2800	1480
2θ scan range [°]	$5.58 < 2\theta < 60.62$	$5.40 < 2\theta < 60.64$	$5.46 < 2\theta < 60.66$	$5.26 < 2\theta < 60.68$	$6.64 < 2\theta < 60.68$
no. of unique data	11796	13011	5903	20122	4136
no. of data obsd [$I > 2\sigma(I)$]	6984	6695	2701	11691	3216
absorption correction	numerical, 13 crystal faces	numerical, 16 crystal faces	numerical, 11 crystal faces	numerical, 21 cryst. faces	numerical, 21 cryst. faces
solution method	Patterson	Patterson	Patterson	Patterson	Patterson
no. of parameters refined	478	490	193	602	154
R , $wR2$ (all data)	0.0743, 0.0551	0.0829, 0.0654	0.0912, 0.0701	0.0921, 0.1554	0.0584, 0.1250
R , (obsd) [a]	3.18	3.59	3.41	5.79	5.20
goodness-of-fit	0.933	1.040	1.014	1.009	1.018

[a] $R1 = \Sigma(F_o - F_c)/\Sigma F_o$; $I > 2\sigma(I)$; $wR2 = \{\Sigma w(F_o^2 - F_c^2)^2/\Sigma w(F_o^2)^3\}^{1/2}$.

4136 were unique after data reduction ($R_{\text{int}} = 0.0597, 0.0612, 0.0721, 0.0897$, and 0.115%). For the numerical absorption correction 13, 16, 11, 21, and 21 indexed crystal faces were used.

In general, the structures were solved with an incomplete data set while the measurement was still being performed, just to confirm the proposed chemical formula, or to find additional solvent molecules that cocrystallized with the compound under investigation. The corrected formula was then used for the final numerical absorption correction. All these procedures were calculated by using Stoe IPDS software.^[31]

The structures were solved with the merged unique data set after checking for correct space groups. Patterson methods were used to solve the crystal structures by applying the software options of the program SHELXS-97.^[32] All structure refinements were performed with the program SHELXL-97^[33] PLATON^[34] and PLUTON were also used in the refinements.^[35] The important crystallographic data are collected in Table 2. While the structures of **1**, **2**, **3**, and **5** crystallize in centrosymmetric space groups, the noncentrosymmetric structure of **4** is merohedrally twinned, and Flack's x -parameter^[36] was refined to 0.34(3).

Computational procedures: The unrestricted density functional calculations utilized the ADF program package, version 2000.01,^[37] and were based on the local exchange-correlation potential by Vosko^[38] et al., augmented in a self-consistent manner with Becke's^[39] exchange gradient correction and Perdew's^[40] correlation gradient correction. H and C atoms were described by a double ζ STO basis including one polarization function, whereas for Mn a triple ζ STO basis with one additional 4p function was used (ADF basis sets III and IV, respectively).

CCDC-167740 (**1**), CCDC-167741 (**2**), CCDC-167742 (**3**), CCDC-167743 (**4**), CCDC-167744 (**5**) contain the supplementary crystallographic data for this paper. These data can be obtained free of charge at www.ccdc.cam.ac.uk/contents/retrieving.html (or from the Cambridge Crystallographic Data Centre, 12 Union Road, Cambridge CB2 1EZ, UK; fax: (+44) 1223-336-033; or e-mail: deposit@ccdc.cam.ac.uk).

Acknowledgements

Financial support from the Swiss National Science Foundation (SNSF) is gratefully acknowledged. We thank Dr. P. Burger for preparation of Figure 5a.

- [1] a) E. O. Fischer, H. Leipfinger, *Z. Naturforsch. B* **1955**, *10*, 353; b) G. Wilkinson, F. A. Cotton, J. M. Birmingham, *J. Inorg. Nucl. Chem.* **1956**, *2*, 95.
- [2] a) J. W. Rabalais, L. Karlsson, K. Siegbahn, L. O. Werme, T. Bergman, M. Hussain, *J. Chem. Phys.* **1972**, *57*, 1185; b) S. Evans, M. L. H. Green, B. Jewitt, G. H. King, A. F. Orchard, *J. Chem. Soc. Faraday Trans.* **1974**, *2*, 356; c) C. Cauletti, J. C. Green, M. R. Kelly, P. Powell, J. Vantilborg, J. Robbins, J. Smart, *J. Electron. Spectrosc. Relat. Phenom.* **1980**, *19*, 327.
- [3] M. E. Switzer, R. Wang, M. F. Rettig, A. H. Maki, *J. Am. Chem. Soc.* **1974**, *96*, 7666.
- [4] a) J. H. Ammeter, R. Bucher, N. Oswald, *J. Am. Chem. Soc.* **1974**, *96*, 7833; b) J. H. Ammeter, *J. Magn. Reson.* **1978**, *30*, 299.
- [5] a) N. Hebedanz, F. H. Köhler, G. Müller, J. Riede, *J. Am. Chem. Soc.* **1986**, *108*, 3281; b) D. Cozak, F. Gauvin, J. Demers, *Can. J. Chem.* **1986**, *64*, 71; c) F. H. Köhler, B. Schlesinger, *Inorg. Chem.* **1992**, *31*, 2853.
- [6] W. Bünder, E. Weiss, *Z. Naturforsch. B* **1978**, *33*, 1235.
- [7] A. Almenningen, A. Haaland, S. Samdal, *J. Organomet. Chem.* **1978**, *149*, 219.
- [8] M. E. Switzer, M. F. Rettig, *J. Chem. Soc. Chem. Commun.* **1972**, 687.
- [9] E. O. Fischer, R. Jira, *Z. Naturforsch. B* **1954**, *9*, 618.
- [10] H. Werner, B. Juthani, *J. Organomet. Chem.* **1977**, *129*, C39.
- [11] a) S. Kheradmandan, K. Heinze, H. W. Schmalle, H. Berke, *Angew. Chem.* **1999**, *111*, 2412; *Angew. Chem. Int. Ed.* **1999**, *38*, 2270; b) S. Kheradmandan, V. V. Krivykh, K. Heinze, H. W. Schmalle, H. Berke, *Chimia* **1998**, *52*, 453; c) S. Kheradmandan, H. W. Schmalle, P. Burger, H. Berke, *Chimia* **1999**, *53*, 354; d) S. Kheradmandan, H. W. Schmalle, H. Berke, *ICCC34, Royal Soc. Chem., Dalton Division* **2000**, P0305; e) V. V. Krivykh, I. L. Eremenko, D. Veghini, I. A. Petruneko, D. L. Pountney, D. Unseld, H. Berke, *J. Organomet. Chem.* **1996**, *511*, 111; f) D. Unseld, V. V. Kryvikh, K. Heinze, F. Wild, G. Artus, H. W. Schmalle, H. Berke, *Organometallics* **1999**, *18*, 1525.
- [12] C. G. Howard, G. S. Girolami, G. Wilkinson, M. Thornton-Pett, M. B. Hursthouse, *J. Am. Chem. Soc.* **1984**, *106*, 2033.
- [13] F. H. Köhler, N. Hebedanz, G. Müller, U. Thewalt, B. Kannellakopoulos, R. Kienze, *Organometallics* **1987**, *6*, 115.
- [14] S. Kheradmandan, Thesis, Universität Zürich, 2001.
- [15] a) P. Jutzi, *Chem. Unserer Zeit* **1999**, *33*, 342; b) P. Jutzi, N. Burford, *Chem. Rev.* **1999**, *99*, 969.
- [16] Examples for mononuclear first-row transition metal [MCp₃] complexes include: a) TiCp₃: C. R. Lucas, M. L. H. Green, M. R. A. Forder, K. W. Prout, *J. Chem. Soc. Chem. Commun.* **1973**, 97; b) VCp₃: F. W. Siegert, H. J. D. Meijer, *J. Organomet. Chem.* **1968**, *15*, 131.
- [17] S. Harder, *Coord. Chem. Rev.* **2000**, *199*, 331.
- [18] a) D. J. Burkey, T. P. Hanusa, *Comments Inorg. Chem.* **1995**, *17*, 41; b) A. J. Bridgeman, *J. Chem. Soc. Dalton Trans.* **1997**, 2887.
- [19] a) A. F. Wells, *Acta Crystallogr.* **1954**, *7*, 535; b) A. F. Wells, *Acta Crystallogr.* **1954**, *7*, 545.
- [20] A. F. Wells, *Three-Dimensional Nets and Polyhedra*, Wiley-Interscience, New York, **1977**.
- [21] a) R. E. Dinnebier, F. Olbrich, G. M. Bendele, *Acta Crystallogr. Sect. C* **1997**, *53*, 699; b) S. Neander, U. Behrens, F. Olbrich, *J. Organomet. Chem.* **2000**, *604*, 59.
- [22] P. S. Tanner, J. S. Overby, M. M. Henein, T. P. Hanusa, *Chem. Ber./Recl.* **1997**, *130*, 155.
- [23] J. C. Smart, J. L. Robbins, *J. Am. Chem. Soc.* **1978**, *100*, 3936.
- [24] J. Mason, *Multinuclear NMR*, Plenum Press, New York, USA, **1989**, Chapt. 7, p. 196.
- [25] S. Harder, M. H. Prosenc, *Angew. Chem.* **1996**, *108*, 101; *Angew. Chem. Int. Ed. Engl.* **1996**, *35*, 97.
- [26] B. F. Abrahams, S. R. Batten, H. Hamit, B. F. Hoskins, R. Robson, *Chem. Commun.* **1996**, 1313.
- [27] C. J. Kepert, M. J. Rosseinsky, *Chem. Commun.* **1998**, 31.
- [28] S. R. Batten, R. Robson, *Angew. Chem.* **1998**, *110*, 1558; *Angew. Chem. Int. Ed.* **1998**, *37*, 1461.
- [29] C. B. Aakeroy, A. M. Beatty, B. A. Helfrich, *J. Chem. Soc. Dalton Trans.* **1998**, 1943.
- [30] S. Decurtins, H. W. Schmalle, R. Pellaux, P. Schneuwly, A. Hauser, *Inorg. Chem.* **1996**, *35*, 1451.
- [31] Stoe IPDS Software, Version 2.92; Stoe and Cie, Darmstadt, 1999.
- [32] G. M. Sheldrick, *Acta Crystallogr. Sect. A* **1990**, *46*, 467.
- [33] G. M. Sheldrick, SHELXL97, University of Göttingen, Germany, **1997**.
- [34] A. L. Spek, *Acta Crystallogr. Sect. A* **1990**, *46*, C34.
- [35] A. L. Spek, PLUTON, University of Utrecht, The Netherlands, **1997**.
- [36] H. D. Flack, *Acta Crystallogr. Sect. A* **1983**, *39*, 876.
- [37] a) E. J. Baerends, P. Ros, *Chem. Phys.* **1975**, *8*, 241; b) L. Versluis, T. Ziegler, *J. Chem. Phys.* **1988**, *88*, 322; c) G. te Velde, E. J. Baerends, *J. Comp. Phys.* **1992**, *99*, 84; d) C. Guerra, J. G. Snijders, G. te Velde, E. J. Baerends, *Theor. Chem. Acc.* **1998**, *99*, 391.
- [38] S. H. Vosko, M. Wilk, M. Nusair, *Can. J. Phys.* **1980**, *58*, 1200.
- [39] A. D. Becke, *Phys. Rev. A* **1988**, *38*, 3098.
- [40] J. P. Perdew, *Phys. Rev. B* **1986**, *33*, 8822.

Received: October 8, 2001
Revised: February 14, 2002 [F3599]